Available online at www.sciencedirect.com
ScienceDirect
Nuclear Physics B 851 (2011) 289–297
NUCLEAR PHYSICS B
www.elsevier.com/locate/nuclphysb

Anomalous single production of fourth generation t' quarks at ILC and CLIC

A. Senol *, A.T. Tasci, F. Ustabas

Department of Physics, Kastamonu University, 37100, Kastamonu, Turkey

Received 3 May 2011; received in revised form 24 May 2011; accepted 26 May 2011

Available online 2 June 2011

Abstract

We present a detailed study of the anomalous single fourth generation t' quark production within the dominant Standard Model (SM) decay modes at future e^+e^- colliders. We calculate the signal and background cross sections in the mass range 300–800 GeV. We also discuss the limits of $t'q\gamma$ and $t'qZ$ ($q = u, c$) anomalous couplings as well as values of attainable integrated luminosity for 3σ observation limit.
© 2011 Elsevier B.V. All rights reserved.

1. Introduction

As it is well known that Standard Model (SM) of particle physics includes three generation of fermions, but does not rule out a fourth generation. The only restriction of the fermion generation numbers comes from asymptotic freedom constraint in QCD is less than nine. On the other hand, the bounds from reanalyzed electroweak precision measurements has shown that existence of fourth fermion generations is not prohibited [1,2]. Therefore, the SM can be simply extended with a sequential repetition as four quark and four lepton left-handed doublets and corresponding right-handed singlets.

A possible fourth generation may play an important role in understanding the well-known unanswered questions such as the CP violation and flavor structure of standard theory [3–9], electroweak symmetry breaking [10–13], hierarchies of fermion mass spectrum and mixing angle

* Corresponding author.
E-mail addresses: asenol@kastamonu.edu.tr (A. Senol), atasci@kastamonu.edu.tr (A.T. Tasci), fatmaustbs@gmail.com (F. Ustabas).

0550-3213/$ – see front matter © 2011 Elsevier B.V. All rights reserved.
doi:10.1016/j.nuclphysb.2011.05.022

in quark/lepton sectors [14–18]. Also, the theoretical and experimental aspects of fourth SM generation in a recent review can be found in Ref. [19].

So far, the current 95% C.L. mass lower limits of the fourth generation quarks from experimental measurements at the Tevatron are $m_{t'} > 311$ GeV [20] and $m_{b'} > 338$ GeV [21], whereas the partial wave unitarity gives an upper bound of about 600 GeV [22].

The determination of allowed parameter space of fourth generation fermions will be an important goal of the LHC era. Masses of the fourth generation quarks will already be well known from the LHC data before a TeV scale linear collider runs, since (if they exist) they are predicted to be produced in pairs at the LHC [23]. The large value of their masses would provide special advantage to new interactions originating at a higher scale. The precise determination of fourth generation quark properties may present the existence of physics beyond the SM. The fourth generation quarks can couple to the gauge bosons via new interactions as well as the flavor changing neutral current (FCNC) interactions with anomalous couplings as $t'qV$ ($V = \gamma, Z, g$; $q = u, c$). The FCNC vertices can be described by an effective Lagrangian which contains series in power of κ/Λ where κ is the anomalous magnetic moment type coupling and Λ is the cut off scale of new interactions. Nevertheless, the LHC may not provide us with sufficient information about some parameters of the fourth generation quarks. But, a linear collider with energies on the TeV scale, extremely high luminosity and clean experimental environment, can provide complementary information for these parameters with performing precision measurements that would complete the LHC results. Most popular proposed linear colliders with energies on the TeV scale and extremely high luminosity are International Linear Collider (ILC) [24] and Compact Linear Collider (CLIC) [25]. Due to the anomalous interactions serious contributions can be expected for the production of the fourth generation fermions. These anomalous effects of the fourth generation quarks has been studied in phenomenological perspective at hadron colliders [26–30] and also at future ep colliders [31,32]. In this study, we investigate the single production of fourth generation t' quarks at proposed linear colliders via anomalous interactions. After its production, we assume the dominant SM t' decay channel as $t' \to Wb$. The aim of this study is to find discovery potential of t' parameters from a detailed analysis for signal and background including Monte Carlo simulation. Thus, we implement the related interaction vertices into the CompHEP package [33] and study the FCNC parameters in detail as well as the effects of initial state radiation (ISR) and beamstrahlung (BS) in the e^+e^- collisions.

2. Interactions of fourth generation t' quarks

Before examining the single productions of the t' quarks, an extension the SM with fourth generation is needed. One of the approach for an extension of the SM is simply to add a sequential fourth family fermions where left-handed components transform as a doublet of $SU(2)_L$ and right-handed components as singlets. The interaction of fourth generation t' quarks with three known generation of quarks, q_i, via the SM gauge bosons ($\gamma, g, Z^0, W^\pm$) is given by

$$\begin{aligned} L_s = & -g_e Q_{t'} \bar{t}' \gamma^\mu t' A_\mu \\ & - g_s \bar{t}' T^a \gamma^\mu t' G^a_\mu \\ & - \frac{g}{2c_W} \bar{t}' \gamma^\mu \left(g_V - g_A \gamma^5\right) t' Z^0_\mu \\ & - \frac{g}{2\sqrt{2}} V_{t'q_i} \bar{t}' \gamma^\mu \left(1 - \gamma^5\right) q_i W^\pm_\mu + \text{h.c.} \end{aligned} \tag{1}$$

where g_e, g are the electro-weak coupling constants, and g_s is the strong coupling constant. A_μ, G_μ, Z^0_μ and $W^\pm_\mu$ are the vector fields for photon, gluon, Z^0 boson and $W^\pm$ boson, respectively. $Q_{t'}$ is the electric charge of fourth family quark t'; T^a are the Gell–Mann matrices. g_V and g_A are the vector and axial-vector type couplings of the neutral weak current with t' quark, θ_W is the weak mixing angle and $c_W = \cos\theta_W$. Finally, the $V_{t'q}$ denotes the elements of extended 4×4 CKM mixing matrix which are constrained by flavor physics. In this study, we use the parametrization of extended CKM matrix elements, $V_{t'd} = 0.0044$, $V_{t's} = 0.114$ and $V_{t'b} = 0.22$ [34]. We calculate the decay width of t' via $t' \to Wq$ process as

$$\Gamma\left(t' \to Wq\right) = \frac{\alpha_e^2 |V_{t'q_i}|^2}{16 s_W^2 m_{t'}^3 M_W^2}\left\{m_{t'}^6 - 3m_{t'}^2 M_W^4 + 2M_W^6\right\} \tag{2}$$

where $s_W = \sin\theta_W$, $g = g_e/s_W$, $g_e = \sqrt{4\pi\alpha_e}$ and M_W is the mass of W boson.

In the SM, FCNC interactions are absent at tree level. However, top quark sector is suitable for searching anomalous FCNC interactions as being heaviest particle to date discovered [35]. The fourth generation t' quarks which are heavier than the top quark can also couple to the FCNC currents. The effective Lagrangian for the anomalous magnetic moment type interactions among the fourth family quarks t', ordinary quarks q, and the neutral gauge bosons $V = \gamma, Z, g$ are given by

$$\begin{aligned} L_a = &\sum_{q_i=u,c,t} \frac{\kappa_\gamma^{q_i}}{\Lambda} Q_{q_i} g_e \bar{t}' \sigma_{\mu\nu} q_i F^{\mu\nu} + \sum_{q_i=u,c,t} \frac{\kappa_Z^{q_i}}{2\Lambda} \frac{g}{c_W} \bar{t}' \sigma_{\mu\nu} q_i Z^{\mu\nu} \\ &+ \sum_{q_i=u,c,t} \frac{\kappa_g^{q_i}}{2\Lambda} g_s \bar{t}' \sigma_{\mu\nu} \lambda_a q_i G_a^{\mu\nu} + \text{h.c.} \end{aligned} \tag{3}$$

where $F^{\mu\nu}$, $Z^{\mu\nu}$ and $G^{\mu\nu}$ are the field strength tensors of the gauge bosons; $\sigma_{\mu\nu} = i(\gamma_\mu\gamma_\nu - \gamma_\nu\gamma_\mu)/2$; λ_a are the Gell–Mann matrices; Q_{q_i} is the electric charge of the quark (q). κ_γ, κ_Z and κ_g are the anomalous couplings with photon, Z boson and gluon, respectively. Λ is the cut-off scale for the new interactions.

Anomalous decay widths of t' quarks which are calculated by using the effective Lagrangian are given below

$$\Gamma\left(t' \to q\gamma\right) = \frac{\kappa_\gamma^2}{2\Lambda^2} \alpha_e Q_{q_i}^2 m_{t'}^3, \tag{4}$$

$$\Gamma\left(t' \to qg\right) = \frac{\kappa_g^2}{3\Lambda^2} \alpha_s m_{t'}^3, \tag{5}$$

$$\Gamma\left(t' \to qZ\right) = \frac{\kappa_Z^2 \alpha_e}{16 m_{t'}^3 \Lambda^2 s_W^2 c_W^2}\left(2m_{t'}^6 - 3M_Z^2 m_{t'}^4 + M_Z^6\right) \tag{6}$$

where M_Z is the mass of the Z boson. All numerical calculations have been performed with CompHEP [33] by including the new interaction vertices. In Table 1, we give the numerical values of the total decay widths and branching ratios for all decay channels of t' quarks by $\kappa_\gamma/\Lambda = \kappa_Z/\Lambda = \kappa_g/\Lambda = 0.1$ TeV^{-1}.

The contributing Feynman Diagrams for anomalous single t' produced in e^+e^- collision are shown in Fig. 1. The analytical expression for cross section of $e^+e^- \to t'q$ $(q = u, c)$ process, calculated by using Lagrangian L_a, is found as

Table 1
Total decay widths (GeV) and branching ratios (%) of the t' quarks in both chiral and anomalous interactions.

$m_{t'}$ (GeV)	Wd	Wb	Ws	$Zu(c)$	Zt	$gu(c)$	gt	$\gamma u(c)$	γt	Γ_{tot} (GeV)
300	0.029	72	19	0.22	0.024	3.6	1.0	0.079	0.023	0.59
400	0.029	71	19	0.23	0.10	3.5	1.9	0.078	0.041	1.43
500	0.028	71	19	0.23	0.15	3.5	2.3	0.077	0.052	2.82
600	0.028	71	19	0.23	0.17	3.5	2.6	0.077	0.059	4.89
700	0.028	70	19	0.24	0.19	3.4	2.8	0.077	0.063	7.79
800	0.028	70	19	0.24	0.20	3.4	3.0	0.076	0.066	11.6

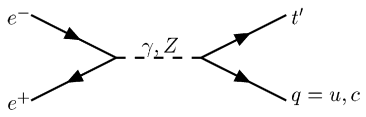

Fig. 1. Feynman diagram for single production of t' in e^+e^- collision.

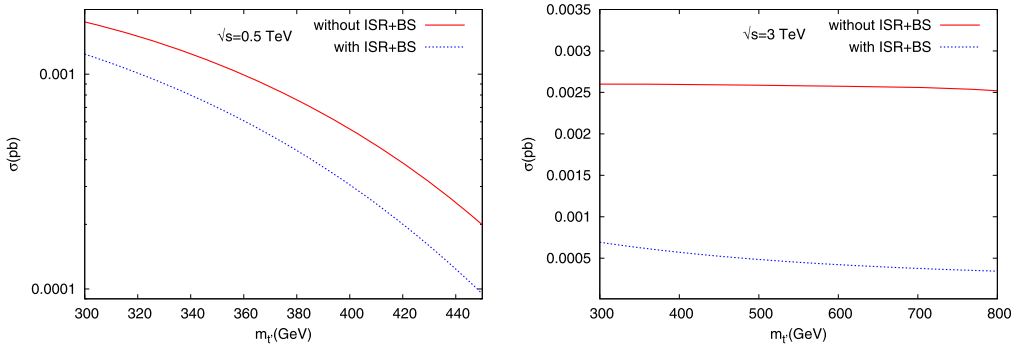

Fig. 2. The total cross sections in pb for the process $e^+e^- \to t'q$ $(q = u, c)$, as function of m'_t at (a) $\sqrt{s} = 0.5$ TeV and (b) $\sqrt{s} = 3$ TeV.

$$\sigma = \frac{\pi\alpha_e^2(2m_{t'}^6 - 3m_{t'}^4 s + s^3)}{48s_W^4 c_W^4 \Lambda^2 s^3[(s - M_Z^2)^2 + \Gamma_Z^2 M_Z^2]}\Big[9s^2\big(1 - 4s_W^2 + 8s_W^4\big)\kappa_Z^2 + 48s_W^2 c_W^2 \kappa_Z \kappa_\gamma \big(1 - 4s_W^2\big)s\big(s - M_Z^2\big) + 128s_W^4 c_W^4 \kappa_\gamma^2\big(\big(s - M_Z^2\big)^2 + \Gamma_Z^2 M_Z^2\big)\Big] \tag{7}$$

where Γ_Z is the total decay width of Z boson.

3. Signal and background analysis

The total cross sections for single production of t' quarks are plotted in Fig. 2 with respect to their masses at collision center of mass energies (a) 0.5 TeV and (b) 3 TeV with assumption $\kappa/\Lambda = 0.1$ TeV^{-1}. A specific feature of the linear colliders is the occurrence of initial state radiation (ISR) and beamstrahlung (BS). When calculating the ISR and BS effects, we take beam parameters which are given in Table 2 for the ILC and CLIC. In Fig. 2, the dotted line denotes the cross section including ISR + BS effects while solid line denotes without ISR + BS effects. The effects of ISR and BS can lead to a decrease in the cross section. After this point, we take into

Table 2
Main parameters of ILC and CLIC. Here N is the number of particles in bunch. σ_x and σ_y are beam sizes, σ_z is the bunch length.

Parameters	ILC	CLIC
$E_{cm}(\sqrt{s})$ TeV	0.5	3
L (10^{34} cm^{-2} s^{-1})	2	5.9
N (10^{10})	2	0.372
σ_x (nm)	640	45
σ_y (nm)	5.7	1
σ_z (μm)	300	44

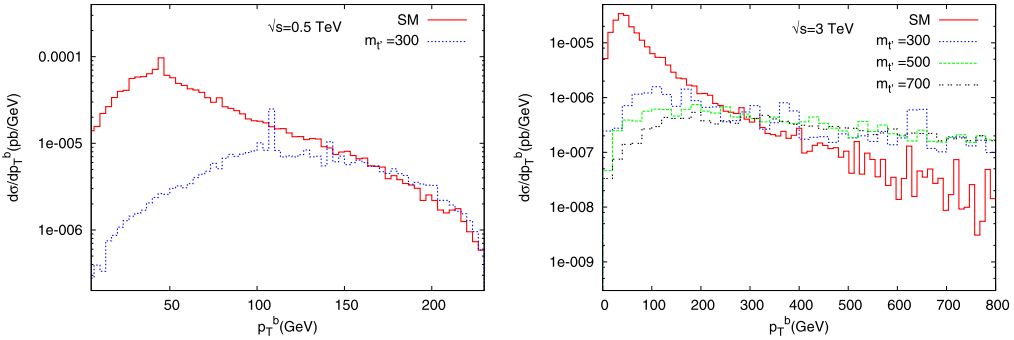

Fig. 3. The differential cross section depending on the transverse momentum of the final state b quark of process $e^+e^- \to W^+bq$ $(q = u, c)$ for SM background (solid line) and signal with different mass values of t' quarks at (a) $\sqrt{s} = 0.5$ TeV and (b) $\sqrt{s} = 3$ TeV.

account ISR + BS effects in all our numerical calculations. The single production of fourth generation t' quarks of signal process including dominance of the SM decay mode over anomalous decay is

$$e^+e^- \to t'q_i \to W^+q_jq_i \quad (q_i = u, c;\ q_j = d, s, b). \tag{8}$$

The transverse momentum (p_T) distributions of the final state b quark for signal and background are shown in Fig. 3 for ILC and CLIC options. Comparing the signal p_T distribution of b quark with that of the corresponding background, we applied a p_T cut of $p_T > 50$ GeV to reduce the background.

The rapidity distributions of final state b quark in signal and background processes are plotted in Fig. 4. From these figures, we can see that the cut $|\eta^b| < 2$ can be applied to suppress the background while the signal remains almost unchanged. We plot the invariant mass distributions for the W^+b system in the final state, the signal has a peak around mass of t' quark over the background as shown in Fig. 5.

In order to discuss the observability of the fourth generation t' quarks at linear colliders, we need to calculate signal and background cross sections as well as the Statistical Significance (SS) which are given in Tables 3 and 4 for ILC and CLIC parameters, respectively. We obtain the SS of the signal by using the formula [36],

$$SS = \sqrt{2L_{int}\epsilon\big[(\sigma_S + \sigma_B)\ln(1 + \sigma_S/\sigma_B) - \sigma_S\big]}.$$

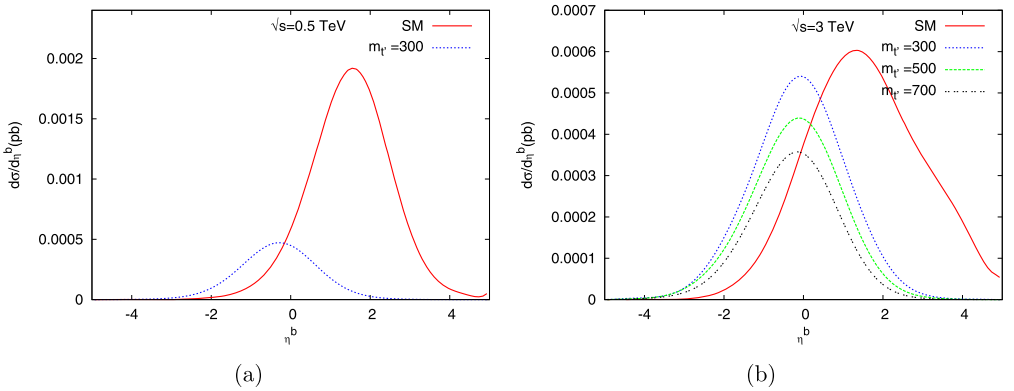

Fig. 4. The rapidity distribution of the final state b quark of the process $e^+e^- \to W^+bq$ $(q = u, c)$ at (a) $\sqrt{s} = 0.5$ TeV and (b) $\sqrt{s} = 3$ TeV.

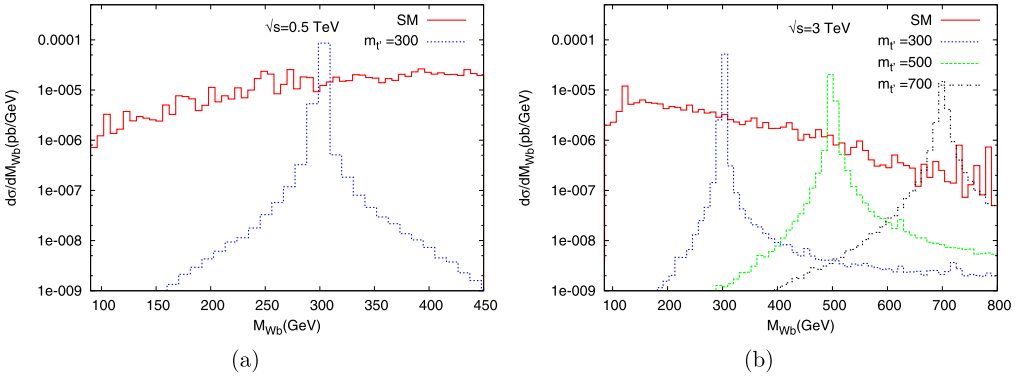

Fig. 5. The invariant mass distribution of the final state Wb system for SM background (solid line) and signal from t' decay for (a) $m_{t'} = 300$ GeV (dotted line) at $\sqrt{s} = 0.5$ TeV and (b) $m_{t'} = 300$ GeV (dotted line), $m_{t'} = 500$ GeV (dashed line) and $m_{t'} = 700$ GeV (dot-dashed line) at $\sqrt{s} = 3$ TeV.

Table 3
The signal and background cross sections in pb and signal Statistical Significance (SS) for the ILC at $\sqrt{s} = 0.5$ TeV with integrated luminosity of 2×10^5 pb^{-1} by assuming $\kappa_\gamma/\Lambda = \kappa_Z/\Lambda = \kappa_g/\Lambda = 0.1$ TeV^{-1}.

$m_{t'}$ (GeV)	σ_S (pb)	σ_B (pb)	SS
300	1.17×10^{-3}	5.08×10^{-5}	10.92
350	7.88×10^{-4}	9.69×10^{-5}	7.17
400	3.95×10^{-4}	1.58×10^{-4}	3.62
450	9.09×10^{-5}	2.05×10^{-4}	0.88

where σ_S and σ_B are the signal and background cross sections, respectively. For realistic analysis we take into account finite energy resolution of the detectors. We use the mass bin width $\Delta m = \max(2\Gamma, \delta m)$ in our numerical calculations to count signal and background events with the mass resolution δm. We also apply the mentioned p_T and η cuts assuming the integrated

Table 4
The signal and background cross sections in pb and signal Statistical Significance (*SS*) for the CLIC at $\sqrt{s} = 3$ TeV with integrated luminosity of 5.9×10^5 pb^{-1} by assuming $\kappa_\gamma/\Lambda = \kappa_Z/\Lambda = \kappa_g/\Lambda = 0.1$ TeV^{-1}.

$m_{t'}$ (GeV)	σ_S (pb)	σ_B (pb)	*SS*
300	1.48×10^{-3}	2.01×10^{-5}	25.68
400	1.27×10^{-3}	1.88×10^{-5}	23.47
500	1.05×10^{-3}	1.77×10^{-5}	20.96
600	1.09×10^{-3}	2.32×10^{-5}	20.62
700	9.55×10^{-4}	2.77×10^{-5}	18.35
800	8.40×10^{-4}	3.17×10^{-5}	16.44

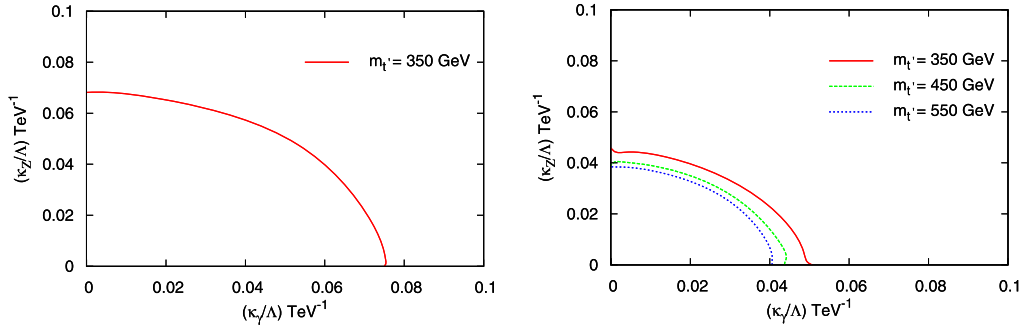

(a) (b)

Fig. 6. The 3σ contour plot for the anomalous couplings reachable at (a) $\sqrt{s} = 0.5$ TeV with $L_{int} = 2 \times 10^5$ pb^{-1} and (b) $\sqrt{s} = 3$ TeV with $L_{int} = 5.9 \times 10^5$ pb^{-1}.

luminosities given in Table 2. Here, we also consider the final state W boson in the signal and background processes decay leptonicaly via $W^\pm \to l^\pm \nu_l$ where $l^\pm = e^\pm, \mu^\pm$ and we assume the b-tagging efficiency as $\epsilon = 50\%$. From Tables 3 and 4, we see that t' quarks can be observed in the scanned mass interval of 300–800 GeV at the CLIC while up to about 400 GeV at the ILC with the observability criteria of 3σ by taking the anomalous couplings $\kappa_\gamma/\Lambda = \kappa_Z/\Lambda = \kappa_g/\Lambda = 0.1$ TeV^{-1}. Up to now, we assume the anomalous couplings are equal to each other. To analyze the case of $\kappa_\gamma/\Lambda \neq \kappa_Z/\Lambda$, the 3σ contour plots for the anomalous couplings in the $\kappa_\gamma/\Lambda - \kappa_Z/\Lambda$ plane are presented in Fig. 6 (a) for $\sqrt{s} = 0.5$ TeV and (b) for $\sqrt{s} = 3$ TeV with different mass values of t' quarks. According to these figures the lower limits of κ_γ/Λ and κ_Z/Λ are about 0.07 TeV^{-1} at the ILC and 0.05 TeV^{-1} at the CLIC energies for $m_{t'} = 350$ GeV. We plot the 3σ contours in the κ/Λ–$m_{t'}$ plane for different masses of t' quarks as shown in Fig. 7. The area of the allowed parameter space of t' quarks are above the lines in Figs. 6 and 7 by taking into account the extended CKM matrix elements.

Finally, in Fig. 8, we plot the lowest necessary luminosities with 3σ observation limits depending on anomalous couplings at (a) $\sqrt{s} = 0.5$ TeV and (b) 3 TeV energies, respectively. It is seen that the fourth generation t' quarks with masses 350 GeV can be observed at 3σ observation limit with lowest integrated luminosity about 3×10^4 pb^{-1} at ILC and CLIC.

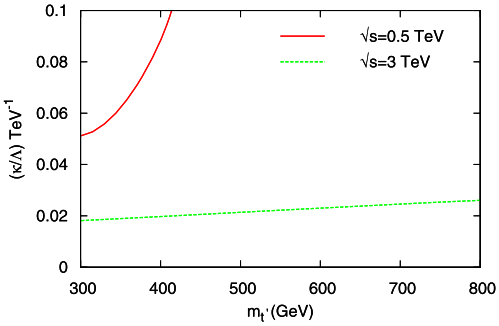

Fig. 7. The 3σ contour plot for the discovery of t' quarks at the center of mass energies of ILC and CLIC with luminosities of 2×10^5 pb^{-1} and 5.9×10^5 pb^{-1}.

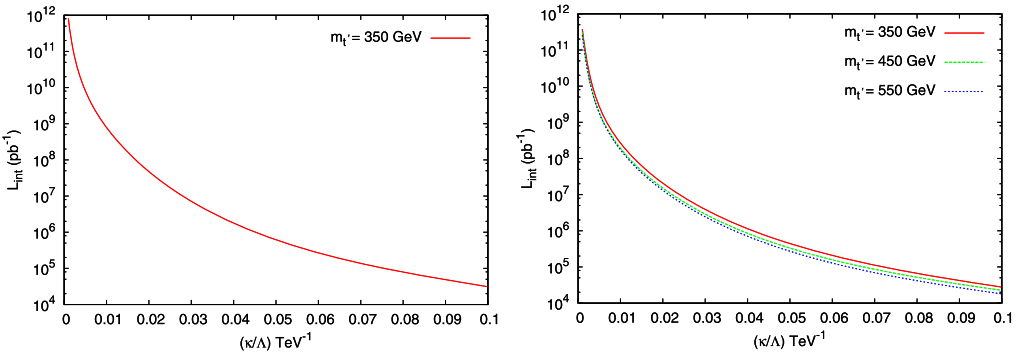

Fig. 8. The attainable integrated luminosity for 3σ observation limit depending on anomalous couplings at (a) $\sqrt{s} = 0.5$ TeV and (b) $\sqrt{s} = 3$ TeV.

4. Conclusion

We find the discovery regions of the parameter space for the single production of fourth generation t' quarks via anomalous interaction vertices at the ILC and CLIC energies. If the fourth generation t' quarks have anomalous couplings that dominate over the SM chiral interactions they can be produced with large numbers. Our results shows that, the lower limit of the anomalous couplings κ_γ/Λ and κ_Z/Λ are found down to 0.07 TeV^{-1} and 0.05 TeV^{-1} for ILC and CLIC, respectively, assuming a maximal parametrization for extended CKM elements. We also find the lowest necessary luminosity limit values for the e^+e^- colliders which will provide a unique opportunity to search for anomalous couplings of the fourth generation t' quarks.

References

[1] H.J. He, N. Polonsky, S.f. Su, Phys. Rev. D 64 (2001) 053004.
[2] G.D. Kribs, T. Plehn, M. Spannowsky, T.M.P. Tait, Phys. Rev. D 76 (2007) 075016.
[3] W.S. Hou, C.Y. Ma, Phys. Rev. D 82 (2010) 036002.
[4] S. Bar-Shalom, D. Oaknin, A. Soni, Phys. Rev. D 80 (2009) 015011.
[5] A.J. Buras, B. Duling, T. Feldmann, T. Heidsieck, C. Promberger, S. Recksiegel, JHEP 1009 (2010) 106.
[6] A. Soni, A.K. Alok, A. Giri, R. Mohanta, S. Nandi, Phys. Lett. B 683 (2010) 302.

[7] O. Eberhardt, A. Lenz, J. Rohrwild, Phys. Rev. D 82 (2010) 095006.
[8] A. Soni, A.K. Alok, A. Giri, R. Mohanta, S. Nandi, Phys. Rev. D 82 (2010) 033009.
[9] A.K. Alok, A. Dighe, D. London, Phys. Rev. D 83 (2011) 073008.
[10] B. Holdom, Phys. Rev. Lett. 57 (1986) 2496;
B. Holdom, Phys. Rev. Lett. 58 (1987) 177 (Erratum).
[11] C.T. Hill, M.A. Luty, E.A. Paschos, Phys. Rev. D 43 (1991) 3011.
[12] T. Elliott, S.F. King, Phys. Lett. B 283 (1992) 371.
[13] P.Q. Hung, C. Xiong, Nucl. Phys. B 848 (2011) 288.
[14] B. Holdom, JHEP 0608 (2006) 076.
[15] P.Q. Hung, M. Sher, Phys. Rev. D 77 (2008) 037302.
[16] P.Q. Hung, C. Xiong, Phys. Lett. B 694 (2011) 430–434.
[17] P.Q. Hung, C. Xiong, Nucl. Phys. B 847 (2011) 160.
[18] O. Cakir, A. Senol, A.T. Tasci, Europhys. Lett. 88 (2009) 11002.
[19] B. Holdom, W.S. Hou, T. Hurth, M.L. Mangano, S. Sultansoy, G. Unel, PMC Phys. A 3 (2009) 4.
[20] A. Lister, CDF Collaboration, arXiv:0810.3349 [hep-ex].
[21] T. Aaltonen, et al., CDF Collaboration, Phys. Rev. Lett. 104 (2010) 091801.
[22] M.S. Chanowitz, M.A. Furman, I. Hinchliffe, Nucl. Phys. B 153 (1979) 402.
[23] ATLAS detector and physics performance technical design report, vol. 2, p. 519, Reports No. CERN-LHCC-99-15 and No. ATLAS-TDR-15, May 1999.
[24] J. Brau, et al. (Eds.), ILC Collaboration, ILC reference design report: ILC global design effort and world wide study, arXiv:0712.1950 [physics.acc-ph].
[25] H. Braun, et al., CLIC Study Team Collaboration, CLIC-NOTE-764, CLIC 2008 parameters.
[26] E. Arik, O. Cakir, S. Sultansoy, Europhys. Lett. 62 (2003) 332–335.
[27] E. Arik, O. Cakir, S. Sultansoy, Phys. Rev. D 67 (2003) 035002.
[28] I.T. Cakir, H. Duran Yildiz, O. Cakir, et al., Phys. Rev. D 80 (2009) 095009.
[29] R. Ciftci, Phys. Rev. D 78 (2008) 075018.
[30] M. Sahin, S. Sultansoy, S. Turkoz, Phys. Rev. D 82 (2010) 051503.
[31] A.T. Alan, A. Senol, O. Cakir, Europhys. Lett. 66 (2004) 657–660.
[32] R. Ciftci, A.K. Ciftci, arXiv:0904.4489 [hep-ph].
[33] A. Pukhov, et al., arXiv:hep-ph/9908288.
[34] W.S.Y. Hou, M. Nagashima, A. Soddu, Phys. Rev. D 76 (2007) 016004.
[35] H. Fritzsch, D. Holtmannspotter, Phys. Lett. B 457 (1999) 186.
[36] G.L. Bayatian, et al., CMS Collaboration, J. Phys. G 34 (2007) 995.